

RELATIVISTIC MHD CYLINDRICAL JETS AND THEIR LINEAR STABILITY*

CHARALAMPOS SINNIS, NEKTARIOS VLAHAKIS

Section of Astrophysics, Astronomy and Mechanics, Physics Department
National and Kapodistrian University of Athens
Panepistimiopolis, 157 84 Zografos, Athens, Greece

*Received 15 April 2022, accepted 6 June 2022,
published online 9 September 2022*

We find cylindrical steady-state jet configurations, which are shaped and carry the traits of the acceleration and collimation processes occurring in the launching region, as governed by the equations of ideal relativistic magnetohydrodynamics (RMHD). The resulting solutions correspond to a two-component structure having a fast propagating inner core surrounded by a slower outer sheath. After we thoroughly present the algorithm to find such steady-state solutions, we study their linear stability. For both axisymmetric and non-axisymmetric modes, we find similar behaviour and typical growth timescales for the instabilities of the order of a few tenths of jet radius light-crossing time.

DOI:10.5506/APhysPolBSupp.15.3-A22

1. Introduction

Astrophysical jets are unambiguously among the most stable objects throughout the cosmos, reaching total lengths which are many times their initial radii. It is also known that there are various kinds of instabilities that are present in these configurations, which are not able to disrupt/destroy the outflows, contrary to laboratory plasma experiments. As a result, there are numerous studies on the stability of these objects trying to clarify this controversy.

In order to study the problem stated above, we utilize a linear stability analysis. This means that we perturb an initial equilibrium configuration and focus on the early stages of the instabilities' evolution. The choice of the initial configuration plays a very important role, as it may filter some kinds of instabilities and allow the development of others. We may have configurations which do not include thermal pressure [1–4] or are purely hydrodynamic [5–7]. In the most general case, we can have both a thermal

* Presented at the 28th Cracow Epiphany Conference on *Recent Advances in Astroparticle Physics*, Cracow, Poland, 10–14 January, 2022.

and magnetic contribution to the jet dynamics [8, 9]. Apart from that, we may focus on more special cases such as jets without current sheets on their surface [10, 11].

This work will focus on a cold, cylindrical magnetised relativistic jet. We present a general methodology to generate the unperturbed jet configuration in Section 2, then we choose our physical requirements and produce the model in Section 3, and finally in Section 4, we showcase and comment on the linear stability analysis of the aforementioned outflow.

2. Derivation of unperturbed jet configuration

Our aim is to derive the behaviour of the physical quantities for outflows which are assumed to be cylindrical and the dynamics dictated by the ideal relativistic magnetohydrodynamics (RMHD) set of equations (see, for example, [12]). The imposed symmetry on the system leads to the dependence of the physical quantities solely on the radius, $\partial_\phi = \partial_z = 0$, while the system is also assumed to be stationary, $\partial_t = 0$. The term ideal imposes that the plasma resistivity is zero and, finally, the outflow is considered to be cold, meaning that the thermal pressure of the jet is zero, $p = 0$, or equivalently, the specific enthalpy equals one, $\xi \equiv 1 + \frac{\Gamma}{\Gamma-1} \frac{p}{\rho} = 1$ (Γ is the polytropic index). The magnetic and electric fields have absorbed $\sqrt{4\pi}$ and we assume that the speed of light and jet's radius are equal to unity ($c = \varpi_j = 1$).

The main task is to derive profiles which are in accordance with the acceleration and collimation processes taking place at the early stages of the outflow, in the vicinity of the central engine. In order to do so, we need to solve the radial component of the momentum equation (force balance)

$$\frac{B_\phi^2 - E^2}{\varpi} - \rho_0 \frac{\gamma^2 V_\phi^2}{\varpi} + \frac{1}{2} \frac{d(B^2 - E^2)}{d\varpi} = 0, \quad (1)$$

where γ is the Lorentz factor, ρ_0 the proper density, \mathbf{V} the velocity, \mathbf{B} and \mathbf{E} the magnetic and electric field, respectively. The magnetic field consists of two components $\mathbf{B} = B_\phi \hat{\phi} + B_z \hat{z}$, the toroidal and z -component. The electric field is derived by Ohm's law, $\mathbf{E} = -\mathbf{V} \times \mathbf{B}$. If we define the squared co-moving magnetic field as F , we may formulate (1) as

$$\frac{F - B_z^2}{\varpi} - \rho_0 \frac{\gamma^2 V_\phi^2}{\varpi} + \frac{d(F/2)}{d\varpi} = 0. \quad (2)$$

We also need Ferraro's law

$$\begin{aligned} \Omega &= \frac{V_\phi}{\varpi} - \frac{V_z}{\varpi} \frac{B_\phi}{B_z} \xrightarrow{\chi = \Omega \varpi} \\ \chi &= V_\phi - V_z \frac{B_\phi}{B_z}, \end{aligned} \quad (3)$$

where Ω is the angular velocity of the field lines and $\chi = \Omega\varpi$ the radius measured in the light cylinder length unit. This equation connects the physical quantities' profiles with the rotation at the base [12, 13]. Among the physical quantities, we will impose a desired behaviour only on the velocity toroidal component

$$V_\phi = \frac{\lambda\chi}{1 + \lambda\chi^2}, \quad (4)$$

where λ is a constant regulating the maximum value of $V_\phi|_{\max} = \sqrt{\lambda}/2$. This choice for V_ϕ ensures that for distances near the axis $\chi \ll 1$, the profile is linear with respect to the radius $V_\phi \sim \chi$ and for distances $\chi \gg 1/\sqrt{\lambda}$ drops as the inverse of the radius $V_\phi \sim 1/\chi$. This is the only assumption for any physical quantity that we need for the rest of the solution. Combining (3) and the definition of the electric field, we get that E can be written as $E = -\chi B_z$. Thus, when we insert (4) into (3) and square the equation, we get

$$\begin{aligned} \left(\frac{V_z}{B_z}\right)^2 [F + B_z^2(\chi^2 - 1)] &= (\chi - V_\phi)^2 \Leftrightarrow \\ \left(\frac{V_z}{B_z}\right)^2 [F + B_z^2(\chi^2 - 1)] &= \chi^2 \left(1 - \frac{\lambda}{1 + \lambda\chi^2}\right)^2, \end{aligned} \quad (5)$$

where we express the toroidal component of the magnetic field through F , $B_\phi^2 = F + B_z^2(\chi^2 - 1)$. If we replace $V_z^2 = 1 - V_\phi^2 - \frac{1}{\gamma^2}$, then (5) becomes

$$\left(1 - \frac{1}{\gamma^2} - \frac{\lambda\chi^2}{1 + \lambda\chi^2}\right)^2 \left[\frac{F}{B_z^2} + (\chi^2 - 1)\right] = \chi^2 \left(1 - \frac{\lambda}{1 + \lambda\chi^2}\right)^2. \quad (6)$$

The unknown of (6) is χ , so obviously, the above equation is polynomial with respect to the variable. In order to bring the equation to a comprehensive form, we algebraically manipulate (6) into

$$\begin{aligned} \chi^6 \left(\frac{\lambda}{\gamma}\right)^2 + \chi^4 \lambda \left[\frac{2 - \lambda}{\gamma^2} - \lambda \frac{F}{B_z^2} \left(1 - \frac{1}{\gamma^2}\right)\right] \\ + \chi^2 \left[\lambda \frac{F}{B_z^2} \left(\lambda - 2 + \frac{2}{\gamma^2}\right) + \frac{1 - 2\lambda}{\gamma^2}\right] + \left(1 - \frac{1}{\gamma^2}\right) \left(1 - \frac{F}{B_z^2}\right) = 0. \end{aligned} \quad (7)$$

Clearly, this form of the equation is much easier to handle. One crucial element is that there are only even powers of χ , meaning that we may reduce the equation to a 3rd degree polynomial of χ^2 . This is really important as any 3rd degree polynomial is always solvable, hence we are able to have a proper solution in all cases. Furthermore, since this cubic equation has real coefficients, there is always at least one real solution.

3. Outflow modelling

Our aim is to produce new jet models as described in the previous section. The only assumption made thus far is only for V_ϕ (4) in order to formulate the equation providing the radial profile of χ . Observing (7), there are also other quantities and parameters we need to specify in order to be able to fully solve the equation numerically.

Hence, we also need to define the behaviour for F , B_z , γ as functions of radius and specify the value for the parameter λ . We try to find configurations having a fast central component, engulfed by a slower one, with different, in general, densities. In terms of asymptotic dependence on the radius, we choose

$$F, B_z \propto \begin{cases} \text{constant, } \varpi \ll \varpi_j \\ 1/\varpi^2, \varpi \rightarrow \varpi_j \end{cases}, \quad \gamma \propto \begin{cases} \text{constant, } \varpi \ll \varpi_j \\ \text{constant, } \varpi \rightarrow \varpi_j \end{cases}. \quad (8)$$

The functions chosen that fulfil the above requirements are

$$F = \frac{B_0^2}{1 + \Delta y^2}, \quad B_z = \frac{B_0}{1 + y^2}, \quad \gamma = \gamma_b + \frac{\gamma_a - \gamma_b}{1 + Ky^2}, \quad (9)$$

where B_0 , K , Δ , γ_a , and γ_b are constants. Particularly, γ_a and γ_b are the values of the Lorentz factor on the axis and the boundary surface of the jet. y is a normalised distance given by $y = \varpi/\varpi_0$. The new unit length, ϖ_0 , can be calculated by (7) for $\varpi \rightarrow 0$ and is given by

$$\varpi_0 = \sqrt{\frac{(2 - \Delta)(1 - 1/\gamma^2)}{(\lambda - 1)^2 - (1 - 1/\gamma^2)}} \frac{1}{\Omega_0}, \quad (10)$$

where Ω_0 is the value of Ω on the axis of the jet. Density distribution is given by (2) solved with respect to ρ_0 . The toroidal component of the magnetic field is provided by $B_\phi = -\sqrt{F + B_z^2(\chi^2 - 1)}$. Finally, we are now able to produce new unperturbed models for every choice of parameter values that we want to study. We analyse one particular set including $\gamma_a = 10$, $\gamma_b = 5$, $\Omega_0 = 100$, $K = 10$, $B_0 = 1$, $\Delta = 0.99$, and $\lambda = 10^{-4}$.

The above selection results to $V_\phi|_{\max} = 0.01$ so that rotation of the plasma is not important, $V_\phi \ll V_z$. The outlook of the model is summarised in Fig. 1. The solution gives a constant profile for Ω near the axis and then drops to much smaller values near the boundary of the outflow. As a result, ρ_0 is constant near the axis going to its maximum value at $\varpi \sim 0.1\varpi_j$ and then drops up until jet's radius attaining a value of $\rho_0|_{\varpi_j} \sim 10^{-4}$.

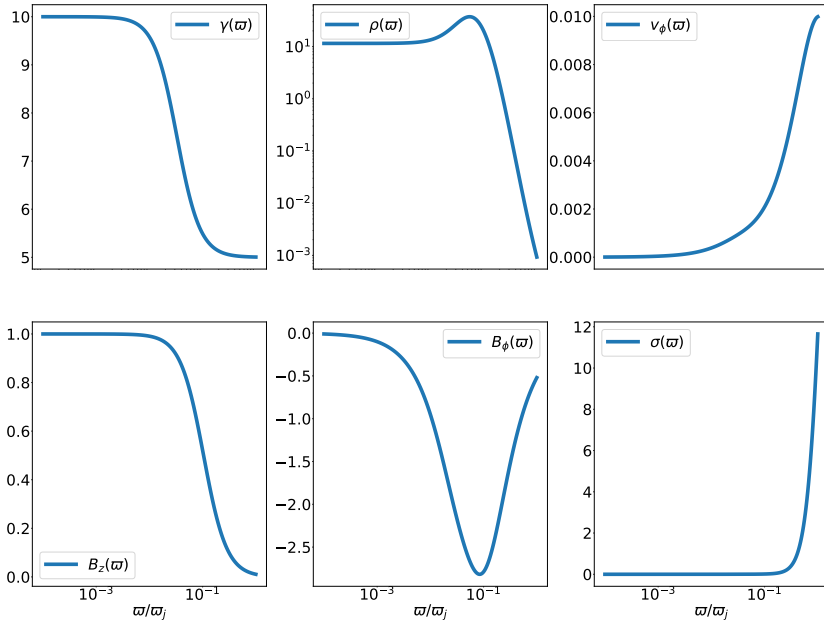


Fig. 1. Plots of the unperturbed jet model generated for the parameters values in Section 3. From left to right, for the top row, we have Lorentz factor, proper density and V_ϕ , while for the bottom row and in the same order, we have B_z , B_ϕ , and magnetisation (σ), respectively.

The magnetisation (σ) is defined as the electromagnetic energy density flow over the kinetic energy density flow, or in the limit where $V_\phi \ll V_z \Rightarrow \sigma \simeq B_\phi^2/(\gamma^2 \rho_0 \xi) \xrightarrow{\text{cold jet}} B_\phi^2/(\gamma^2 \rho_0)$. The jet is kinetically dominated up to $\omega \lesssim 0.1\omega_j$, while for larger distances until the jet's boundary is increasing reaching a maximum value of $\sigma|_{\text{max}} \simeq 12$, corresponding to a magnetically dominated part of the jet. This trend is heavily affected by the decrease in the proper density in the outer region of the outflow.

4. Linear stability analysis

In order to conduct a linear stability analysis of a particular undisturbed cylindrical outflow configuration, we need to insert small perturbations into the RMHD system of equations, linearise, and solve the new system of equations. Thus, for every physical quantity, we perturb $Q(\omega, \phi, z, t) = Q_0(\omega) + \delta Q(\omega, \phi, z, t)$, where $Q_0, \delta Q$ are the unperturbed quantity and the perturbation, respectively. Due to the fact that the configurations are independent of z, ϕ, t , the perturbation can be expressed as $\delta Q(\omega, \phi, z, t) = Q_1(\omega) \exp[i(kz + m\phi - \omega t)]$, where m is integer.

We employ the temporal approach, and thus we choose k real and complex $\omega = \text{Re}(\omega) + i\text{Im}(\omega)$. The perturbation gets the form of $\delta Q(\varpi, \phi, z, t) = Q_1(\varpi) \exp[\text{Im}(\omega)t] \exp[i(kz + m\phi - \text{Re}(\omega)t)]$, which has a time-varying amplitude. For $\text{Im}(\omega) > 0$, the solution is unstable, while for $\text{Im}(\omega) = 0$ and $\text{Im}(\omega) < 0$, the modes are marginally stable and stable, respectively. Apparently, we are solely interested in the unstable modes, so we focus on the positive value range for $\text{Im}(\omega)$. The higher the $\text{Im}(\omega)$ value, the smaller is the corresponding characteristic growth timescale of the instability, $\tau \sim 1/\text{Im}(\omega)$.

There are more steps in order to conduct successfully the linear analysis. These are setting up the environment of the jet, solving the systems of the jet and the environment, and applying the boundary conditions which will provide the dispersion relation plots. A thorough detailed overview of the methodology in the relativistic regime can be found in publications such as [10, 14].

In figure 2, we present the dispersion relation for the model of Section 3. The density ratio η which is the density of the environment over the density on the axis of the jet is set to $\eta = 100$. The general characteristics of the three different dispersion plots are similar. We observe that the maximum values for $\text{Im}(\omega)$ are obtained for $k \lesssim 10$. This is achieved by numerous modes being well localised around a specific k . These modes begin at $k \sim 0.1$ and are present up to the cases that we examine $k \simeq 10$. The trend of these localised solutions continues also for $k > 10$. The values of $\text{Im}(\omega)$ through the various modes increase and reach an upper maximum which is approximately $\text{Im}(\omega)|_{\text{max}} \simeq 0.2$ for all three plots.

As for the solutions which are present over a big range of k , for $m = 0$, the values of $\text{Im}(\omega)$ (red/black thick coloured mode) is below 10^{-4} , a fairly stable mode compared to the others. For $m = \pm 1$, we observe two components, one that peaks at small k and the other at high k . The trend is also the same, so the high- k solutions are more unstable compared to their small wavenumber counterparts, but more stable compared to the localised modes for $k \simeq 8-10$.

Concluding, the prevailing type of instability (maximum $\text{Im}(\omega)$) should be the same for either $m = 0, \pm 1$ since the k values for which they manifest and the corresponding $\text{Im}(\omega)$ are similar. For these solutions, the growth rates that we find are comparable to the ones found in the literature, $\text{Im}(\omega)|_{\text{max}} \sim 0.1$. The modes spanning across the dispersion plot range ($m = \pm 1$) are most probably of electromagnetic nature, as the value of m affects both the shape and the values of $\text{Im}(\omega)$. The axisymmetric case does not showcase a mode similar to the one mentioned above. The localised modes which behave similarly for every dispersion plot hint towards a kinetic instability, most probably Kelvin–Helmholtz due to the difference in

the velocity along the jet axis at the boundary of the outflow. Instabilities based on the rotation of the jet are deemed improbable due to the really small value of V_ϕ .

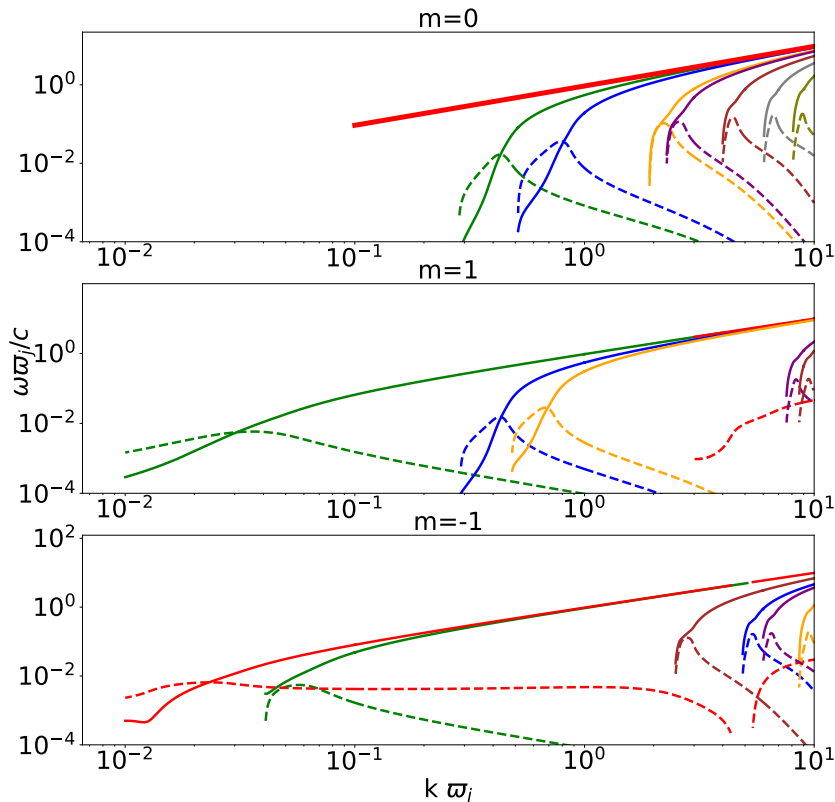


Fig. 2. (Colour on-line) Dispersion plots for the model of Section 3. Plots from top to bottom are for $m = 0, 1, -1$, respectively. Solid lines represent the real part of ω , while dashed lines are the imaginary counterpart. Different modes are represented with different colours. We are interested in the modes having maximum $\text{Im}(\omega)$ at every k of our range as they are the modes which will have the smallest growth timescales and make their impact first on the jet configuration. The unit of ω is the inverse of the jet radius light-crossing time and the unit of k is the inverse of the jet radius.

This research is co-financed by Greece and the European Union (European Social Fund- ESF) through the Operational Programme «Human Resources Development, Education and Lifelong Learning» in the context of the project «Strengthening Human Resources Research Potential via Doctorate Research» (MIS-5000432), implemented by the State Scholarships Foundation (IKY).

REFERENCES

- [1] S. Appl, T. Lery, H. Baty, «Current-driven instabilities in astrophysical jets. Linear analysis», *Astron. Astrophys.* **355**, 818 (2000).
- [2] E. Sobacchi, Y.E. Lyubarsky, M.C. Sormani, «Kink instability of force-free jets: a parameter space study», *Mon. Not. R. Astron. Soc.* **468**, 4635 (2017).
- [3] E. Sobacchi, Y.E. Lyubarsky, «External confinement and surface modes in magnetized force-free jets», *Mon. Not. R. Astron. Soc.* **473**, 2813 (2018).
- [4] R. Narayan, J. Li, A. Tchekhovskoy, «Stability of Relativistic Force-free Jets», *Astrophys. J.* **697**, 1681 (2009).
- [5] A. Ferrari, E. Trussoni, L. Zaninetti, «Relativistic Kelvin–Helmholtz Instabilities in Extragalactic Radio-sources», *Astron. Astrophys.* **64**, 43 (1978).
- [6] H. Cohn, «The stability of a magnetically confined radio jet», *Astrophys. J.* **269**, 500 (1983).
- [7] G. Bodo, A. Mignone, R. Rosner, «Kelvin–Helmholtz instability for relativistic fluids», *Phys. Rev. E* **70**, 036304 (2004).
- [8] A. Ferrari, E. Trussoni, L. Zaninetti, «Magnetohydrodynamic Kelvin–Helmholtz instabilities in astrophysics — II. Cylindrical boundary layer in vortex sheet approximation», *Mon. Not. R. Astron. Soc.* **196**, 1051 (1981).
- [9] G. Bodo, G. Mamatsashvili, P. Rossi, A. Mignone, «Linear stability analysis of magnetized jets: the rotating case», *Mon. Not. R. Astron. Soc.* **462**, 3031 (2016).
- [10] J. Kim, D.S. Balsara, M. Lyutikov, S.S. Komissarov, «On the linear stability of magnetized jets without current sheets — relativistic case», *Mon. Not. R. Astron. Soc.* **467**, 4647 (2017).
- [11] J. Kim, D.S. Balsara, M. Lyutikov, S.S. Komissarov, «On the linear stability of sheared and magnetized jets without current sheets — relativistic case», *Mon. Not. R. Astron. Soc.* **474**, 3954 (2018).
- [12] N. Vlahakis, «Ideal Magnetohydrodynamic Solution to the σ Problem in Crab-like Pulsar Winds and General Asymptotic Analysis of Magnetized Outflows», *Astrophys. J.* **600**, 324 (2004).
- [13] S.S. Komissarov, N. Vlahakis, A. Königl, M.V. Barkov, «Magnetic acceleration of ultrarelativistic jets in gamma-ray burst sources», *Mon. Not. R. Astron. Soc.* **394**, 1182 (2009).
- [14] G. Bodo, G. Mamatsashvili, P. Rossi, A. Mignone, «Linear stability analysis of magnetized relativistic jets: the non-rotating case», *Mon. Not. R. Astron. Soc.* **434**, 3030 (2013).